



Short Communication

Rupture process models of the Yangbi and Maduo earthquakes that struck the eastern Tibetan Plateau in May 2021

Weimin Wang^{a,*}, Jiankun He^a, Xun Wang^b, Yun Zhou^c, Jinlai Hao^d, Lianfeng Zhao^d, Zhenxing Yao^d^a State Key Laboratory of Tibetan Plateau Earth System, Resources and Environment, Institute of Tibetan Plateau Research, Chinese Academy of Sciences, Beijing 100101, China^b Institute of Earthquake Forecasting, China Earthquake Administration, Beijing 100036, China^c Institute of Geophysics, China Earthquake Administration, Beijing 100081, China^d Institute of Geology and Geophysics, Chinese Academy of Sciences, Beijing 100029, China

ARTICLE INFO

Article history:

Received 24 June 2021

Received in revised form 28 October 2021

Accepted 29 October 2021

Available online 7 November 2021

© 2021 Science China Press. Published by Elsevier B.V. and Science China Press. This is an open access article under the CC BY-NC-ND license (<http://creativecommons.org/licenses/by-nc-nd/4.0/>).

An M6.4 earthquake struck Yangbi County, Dali Prefecture, Yunnan Province, on May 21, 2021, at 21:48 Beijing Time (2021-05-21 13:48:37 UTC). Soon thereafter, at 2:04 UTC on May 22, 2021 (2021-05-21 18:04:13 UTC), an M7.4 earthquake struck Maduo County, Guoluo Prefecture, Qinghai Province. These two earthquakes occurred in the southeastern edge and in high-altitude hinterland of the eastern Tibetan Plateau respectively (Fig. 1a), and both caused human casualties and property damage, triggering earthquake emergency response efforts. The occurrence of strong earthquakes at different sites within 5 h of each other indicates continuous tectonic movements and violent seismic activity on the Tibetan Plateau under the collisional convergence between the Indian and Eurasian continental plates [3]. Observations of crustal motion expose clockwise rotational deformation in the eastern Tibetan Plateau along the axis of the eastern Himalayan syntaxis [2,4]. Furthermore, studies combining tectonic and historical seismic data with numerical simulations reveal that the shear effect of the eastward flow of crustal material within the Tibetan Plateau leads to active sinistral strike-slip faulting in the northern part of the plateau and dextral strike-slip faulting in the south [1,3,5]. The source mechanisms of these two events (Fig. S1 online) suggest that both earthquakes occurred in response to the strain induced by the current crustal deformation, which is consistent with the above deformation pattern of the Tibetan Plateau.

Accordingly, studying the deformation mechanisms in and around the Tibetan Plateau, being the largest zone of tectonic deformation on Earth, is a major focus of ongoing geoscience research. Nevertheless, the main views of the two predominant intraplate deformation models, the “block model” and the “continuum model”, cannot perfectly explain the observed deformation

and seismic activity across the Tibetan Plateau [2], indicating that further work is needed. In this context, we developed models of the spatiotemporal source rupture processes of these two strong earthquakes by jointly inverting seismic waveforms and coseismic deformation data, thereby revealing the corresponding tectonic motion characteristics. These findings can provide new insights into and constraints on the deformation mechanisms on the Tibetan Plateau. Additionally, the proposed source models, as fundamental components of seismological research, can provide a scientific basis for seismic hazard mitigation and earthquake risk assessment.

We downloaded waveform records acquired at globally distributed digital seismic stations through the Incorporated Research Institutions for Seismology (IRIS) Data Management Center to rapidly invert the focal mechanisms and source rupture processes of these two strong earthquakes. Based on the preliminary results, we gathered additional observations to construct a finite fault model and accurately obtained the corresponding source processes by a joint inversion. The data used to study the Yangbi earthquake source process are regional three-component waveforms (downloaded from the China National Digital Seismic Network), far-field P and SH waveforms, and coseismic deformation data (interferometric synthetic aperture radar, InSAR) obtained from the European Space Agency (ESA) Sentinel satellites, whose radar images cover the pre- and postearthquake source area (Table S1 online). To study the Maduo earthquake source process, due to the lack of near-source seismic records, we used far-field P and SH waveforms and coseismic line-of-sight (LOS) displacements obtained from the ESA Sentinel satellites. First, the basic parameters of the seismogenic fault, including the hypocenter, strike, dip and rake angle, were determined using the focal mechanism (Fig. 1a) combined with the tectonic background and active fault information [3]. Then, a more accurate geometric model of the fault was

* Corresponding author.

E-mail address: wangwm@itpcas.ac.cn (W. Wang).

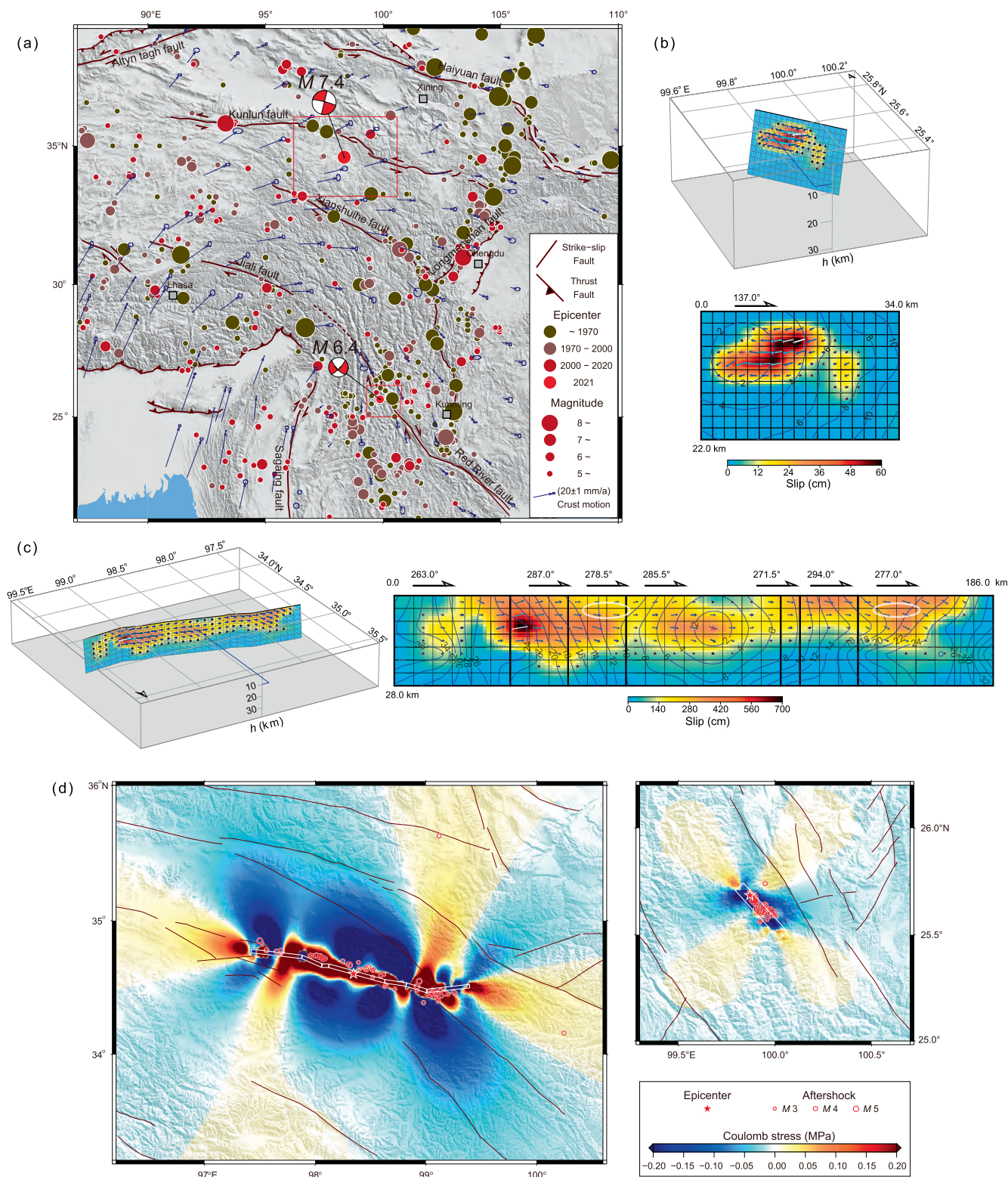


Fig. 1. (a) Tectonic setting of the eastern Tibetan Plateau showing the locations and focal mechanisms of the Yangbi earthquake and Maduo earthquake. Major faults are modified from Ref. [1], and the historical earthquakes are from the National Earthquake Data Center. GPS vectors are from Ref. [2] and are relative to a fixed stable Eurasia. (b) Temporal and spatial distributions of slip on the Yangbi earthquake fault plane (bottom) and a 3D view of the finite fault model (top). (c) Temporal and spatial distributions of slip on the Maduo earthquake fault plane (right) and a 3D view of the finite fault model (left). On the fault plane, the white ellipses indicate the supershear rupture velocities revealed by the rupture front propagation time. (d) Coulomb stress changes due to the coseismic rupture of the Yangbi earthquake (right) and Maduo earthquake (left). Active faults from Ref. [3] are shown as dark red lines. The surface projections of the fault models are shown as white lines.

constructed by using coseismic deformation images (InSAR). The simulated annealing technique was used to finally obtain the earthquake source rupture process models through the joint inversion of the waveforms and coseismic deformation data [6].

For further details about the data processing and calculation (Tables S2 and S3 online), see the Supplementary materials.

To investigate the earthquake rupture processes, we constructed a 34 km (along strike) × 22 km (down-dip) fault plane

composed of 187 (17×11) subfaults of $2 \text{ km} \times 2 \text{ km}$ for the Yangbi earthquake and a 186 km (along strike) \times 28 km (downdip) fault plane composed of 217 (31×7) subfaults of $6 \text{ km} \times 4 \text{ km}$ for the Maduo earthquake. We employed earthquake epicenter locations of (25.67°N , 99.87°E) for the Yangbi earthquake and (34.59°N , 98.34°E) for the Maduo earthquake released by the China Earthquake Networks Center (<http://news.ceic.ac.cn>) as the initial rupture points of the earthquakes. The rupture process model of the Yangbi earthquake was obtained by the joint inversion of regional (13 three-component seismograms), far-field waveforms (14 P waveforms and 21 SH waveforms) and InSAR coseismic displacement data (Figs. S2a, S3a, b, and S4a online). Our results (Fig. 1b) reveal that the source of the Yangbi earthquake was characterized by a unilateral rupture that propagated from northwest to southeast along the fault plane with a source duration of approximately 8 s. The peak slip reached approximately 60 cm, the total seismic moment was approximately $1.8 \times 10^{18} \text{ N m}$, and the magnitude was approximately $M_w6.11$. The Yangbi earthquake was a shallow dextral strike-slip event with a small normal dip-slip component, which is compatible with the strain environment of the crust moving from southeast to southwest as revealed by the GPS velocity field in the source area. Likewise, the rupture process model of the Maduo earthquake was obtained by the joint inversion of far-field waveforms (30 P waveforms and 26 SH waveforms) and InSAR coseismic displacement data (Figs. S2b, S3c, and S4b online), and the results (Fig. 1c) show that the rupture propagated in both directions along the fault plane and produced many surface ruptures. During the eastward propagation of the source rupture, the peak slip value of 682 cm occurred near 99°E , and the strike at the eastern end of the fault was deflected toward the north. During the westward propagation of the source rupture, the peak slip value of 357 cm occurred near 97.8°E , and the strike at the western end of the fault was deflected toward the south. The slip distribution of the Maduo earthquake presents three high-slip zones in the eastern, middle and western parts of the fault plane. The overall rupture was characterized mainly by sinistral strike-slip with a source duration of approximately 36 s. The eastern section exhibited a small thrust component, while the western end displayed a small normal dip-slip component. These rupture features should be related to the changes in the fault strike and local variations in the tectonic environment. We estimated that the total seismic moment of the Maduo earthquake was approximately $2.27 \times 10^{20} \text{ N m}$ and that the magnitude was approximately $M_w7.51$. According to the time contours of rupture propagation, our results also show that the rupture of the Maduo earthquake reached supershear velocities ($>4 \text{ km/s}$) on the eastern and western parts of the fault plane (Fig. 1c). Moreover, the reliability of the inverted rupture process models was estimated using the bootstrap technique (Fig. S5 online), with the calculations reflecting good credibility (see the Supplementary materials).

Earthquake ruptures induce stress changes on neighboring faults that might trigger or suppress subsequent earthquakes [7]. We calculated the Coulomb stress changes produced by the slip distribution models for the Yangbi and Maduo earthquakes [8]. Fig. 1d shows the variation in the Coulomb stress at a depth of 10 km for the Yangbi earthquake and a depth of 20 km for the Maduo earthquake. The distribution of aftershocks up to June 12 after these two strong seismic events (released by the China Earthquake Networks Center) correlates well with the area in which the Coulomb stress increased. The Coulomb stress increased by 0.1 bar on the middle and southern sections of the Weixi-Qiaohou fault (North Red River fault) to the east of the Yangbi earthquake rupture zone and by 0.2 bar on the western part of the Maduo-Gande

fault and the northeastern part of the East Kunlun fault near the Maduo earthquake rupture zone.

The inverted source rupture models demonstrate that the rupture slips of both strong earthquakes occurred in the upper crust within a depth of 20 km beneath the eastern Tibetan Plateau. These features support the existence of low-velocity, high-conductivity, high-attenuation zones of weakness in the lower and middle crust beneath the eastern Tibetan Plateau, and the interpretation of the deformation pattern supports a lower crustal lateral flow model [5,9]. The “block model”, which explains the mechanisms of intra-plate deformation, divides the Tibetan Plateau into rigid blocks, where the velocity of motion within a given block is described by Eulerian polar rotation and elastic strain accumulates near the block boundaries [2,10]. The Yangbi earthquake occurred near the boundary between the Sichuan-Yunnan and Baoshan blocks [3,10], and its magnitude and source mechanism are consistent with the deformation characteristics derived from the “block model”. However, the kinematic features revealed by our Maduo earthquake rupture model, such as the steeply dipping sinistral strike-slip fault, the supershear rupture velocities, and the produced surface ruptures, are very similar to the rupture features of the 2001 Kokoxili $M_w7.9$ earthquake that occurred on the East Kunlun fault and the 2010 Yushu $M_w6.9$ earthquake that occurred on the Xianshuihe fault [11,12]. It is worth noting that the characteristics of the seismogenic fault of the Maduo earthquake fault, namely, its slip rate, interseismic strain and seismic activity, are significantly different from those of the East Kunlun fault and Xianshuihe fault [2], which are deep major faults on the Tibetan Plateau located to the north and south, respectively, of the Maduo epicenter. The Maduo event ruptured the seismogenic fault over hundreds of kilometers within the Bayan Har block, which is usually considered stable. This challenges the existing “block model”. Additionally, the Maduo $M_w7.5$ earthquake occurred in an area where the Coulomb stress caused by the surrounding historical strong earthquakes was negative [13]. Overall, the source rupture process models obtained from this research reveal the accurate and detailed kinematic characteristics of the Yangbi and Maduo earthquakes and provide kinematic constraints that can be used to study the dynamic mechanisms responsible for these two strong earthquakes. Furthermore, combined with knowledge of the rheology, tectonic loading, and fault strength revealed by previous research, these kinematic models can be used to further investigate the deformation mechanisms and assess the earthquake risk on the Tibetan Plateau.

In summary, through the joint inversion of seismic waveforms and InSAR coseismic displacement data, our study revealed the spatiotemporal source rupture processes of the two strong earthquakes that struck the eastern Tibetan Plateau in May 2021. The results show that the Yangbi earthquake, which occurred along the southeastern margin of the Tibetan Plateau, was an $M_w6.1$ event characterized by unilateral dextral strike-slip rupture and an 8 s duration. In addition, the Maduo earthquake, which occurred in the interior of the Tibetan Plateau, was an $M_w7.5$ event characterized by sinistral strike-slip extending along both sides of the seismogenic fault and a 36 s duration. The rupture properties of these two strong earthquakes reflect the deformation characteristics of different parts of the eastern Tibetan Plateau. These events also caused the Coulomb stress of the surrounding active faults to increase, so the risk potential of future earthquakes should be evaluated.

Conflict of interest

The authors declare that they have no conflict of interest.

Acknowledgments

This work was supported by the Second Tibetan Plateau Scientific Expedition and Research Program (2019QZKK0708), the National Natural Science Foundation of China (42120104004, 41974054, and 41904094), and the Strategic Priority Research Program of the Chinese Academy of Sciences (XDA20070302). Some figures were prepared with GMT software [14].

Author contributions

Weimin Wang built the earthquake models and carried out the numerical inversion calculations. Xun Wang processed the InSAR data. Yun Zhou calculated the Coulomb stress. Jinlai Hao and Lianfeng Zhao contributed to the data analyses. Weimin Wang drafted the manuscript. Jiankun He and Zhenxing Yao supervised the research.

Appendix A. Supplementary materials

Supplementary materials to this article can be found online at <https://doi.org/10.1016/j.scib.2021.11.009>.

References

- [1] Tapponnier P, Zhiqin X, Roger F, et al. Oblique stepwise rise and growth of the Tibet Plateau. *Science* 2001;294:1671–7.
- [2] Zheng G, Wang H, Wright T, et al. Crustal deformation in the India-Eurasia collision zone from 25 years of GPS measurements. *J Geophys Res* 2017;122:9290–312.
- [3] Zhang P, Deng Q, Zhang Z, et al. Active faults, earthquake hazards and associated geodynamic processes in continental China. *Sin Earth Terrae* 2013;43:1607–20 (in Chinese).
- [4] Wang Q, Zhang P, Freymueller J, et al. Present-day crustal deformation in China constrained by global positioning system measurements. *Science* 2001;294:574–7.
- [5] Royden L, Burchfiel B, King R, et al. Surface deformation and lower crustal flow in eastern Tibet. *Science* 1997;276:788–90.
- [6] Wang W, Hao J, He J, et al. Rupture process of the Mw7.9 Nepal earthquake April 25 2015. *Sci China Earth Sci* 2015;58:1895–900.
- [7] King G, Stein R, Lin J. Static stress changes and the triggering of earthquakes. *Bull Seismol Soc Am* 1994;84:935–53.
- [8] Okada Y. Internal deformation due to shear and tensile faults in a half-space. *Bull Seism Soc Am* 1992;82:1018–40.
- [9] Zhao L, Xie X, He J, et al. Crustal flow pattern beneath the Tibetan Plateau constrained by regional Lg-wave Q tomography. *Earth Planet Sci Lett* 2013;383:113–22.
- [10] Shen Z, Lu J, Wang M, et al. Contemporary crustal deformation around the southeast borderland of the Tibetan Plateau. *J Geophys Res* 2005;110:B11409.
- [11] Bouchon M, Vallée M. Observation of long supershear rupture during the magnitude 8.1 Kunlunshan earthquake. *Science* 2003;301:824–6.
- [12] Wang D, Mori J. The 2010 Qinghai, China, earthquake: a moderate earthquake with supershear rupture. *Bull Seis Soc Am* 2012;102:301–8.
- [13] Cheng J, Xu X. Features of earthquake clustering from calculation of coulomb stress around the Bayan Har block, Tibetan Plateau. *Seismol Geol* 2018;40:133–54 (in Chinese).
- [14] Wessel P, Smith W. New version of the Generic Mapping Tools released. *Eos Trans AGU* 1995;76:329.



Weimin Wang is an associate professor at the Institute of Tibetan Plateau Research, Chinese Academy of Sciences. His research interest mainly focuses on the earthquake rupture process, seismic wave propagation and attenuation, theoretical seismogram, exploration of earth structure, no-linear optimization.